Taylor & Francis
Taylor & Francis Group

BASIC RESEARCH PAPER

Differing susceptibility to autophagic degradation of two LC3-binding proteins: SQSTM1/p62 and TBC1D25/OATL1

Satoshi Hirano[a], Takefumi Uemura[b], Hiromichi Annoh[b], Naonobu Fujita[a], Satoshi Waguri[b], Takashi Itoh[a,c], and Mitsunori Fukuda[a]

[a]Laboratory of Membrane Trafficking Mechanisms, Department of Developmental Biology and Neurosciences, Graduate School of Life Sciences, Tohoku University, Aobayama, Aoba-ku, Sendai, Miyagi, Japan; [b]Department of Anatomy and Histology, Fukushima Medical University School of Medicine, Fukushima, Japan; [c]Center for Frontier Oral Science, Graduate School of Dentistry, Osaka University, Suita, Osaka, Japan

ABSTRACT

MAP1LC3/LC3 (a mammalian ortholog family of yeast Atg8) is a ubiquitin-like protein that is essential for autophagosome formation. LC3 is conjugated to phosphatidylethanolamine on phagophores and ends up distributed both inside and outside the autophagosome membrane. One of the well-known functions of LC3 is as a binding partner for receptor proteins, which target polyubiquitinated organelles and proteins to the phagophore through direct interaction with LC3 in selective autophagy, and their LC3-binding ability is essential for degradation of the polyubiquitinated substances. Although a number of LC3-binding proteins have been identified, it is unknown whether they are substrates of autophagy or how their interaction with LC3 is regulated. We previously showed that one LC3-binding protein, TBC1D25/OATL1, plays an inhibitory role in the maturation step of autophagosomes and that this function depends on its binding to LC3. Interestingly, TBC1D25 seems not to be a substrate of autophagy, despite being present on the phagophore. In this study we investigated the molecular basis for the escape of TBC1D25 from autophagic degradation by performing a chimeric analysis between TBC1D25 and SQSTM1/p62 (sequestosome 1), and the results showed that mutant TBC1D25 with an intact LC3-binding site can become an autophagic substrate when TBC1D25 is forcibly oligomerized. In addition, an ultrastructural analysis showed that TBC1D25 is mainly localized outside autophagosomes, whereas an oligomerized TBC1D25 mutant rather uniformly resides both inside and outside the autophagosomes. Our findings indicate that oligomerization is a key factor in the degradation of LC3-binding proteins and suggest that lack of oligomerization ability of TBC1D25 results in its asymmetric localization at the outer autophagosome membrane.

Introduction

Macroautophagy (referred to as autophagy below) is the conserved intracellular degradation system in all eukaryotic cells, and it is achieved by the formation and degradation of autophagosomes, which are formed in response to various intracellular stresses, including nutrient starvation, intracellular accumulation of toxic substances, and bacterial intrusions.[1] Autophagy is initiated by the formation of a double-membrane structure called the phagophore in the cytoplasm. The phagophore then elongates and changes into the spherical autophagosome. The resulting autophagosome eventually fuses with endosomes and lysosomes, which results in the degradation of substances within the autophagosome and release of the degradation products, e.g., amino acids, to the cytoplasm. During the past few decades, conserved autophagy-related (ATG) genes whose products are essential for autophagy to occur have been identified in a variety of organisms from yeast to humans.[2,3]

One of the Atg proteins, Atg8, is a ubiquitin-like protein, and, in contrast to the presence of Atg8 alone in yeast, many Atg8 orthologs classified into 2 main subfamilies (i.e., the MAP1LC3/LC3 family, and the GABARAP family) have been identified in mammals. MAP1LC3B/LC3B (simply referred to as LC3 below) is the best characterized representative of the mammalian Atg8 orthologs,[4] and it is conjugated to phosphatidylethanolamine and localized to phagophores by ubiquitin-conjugation-like machinery composed of other ATG proteins.[5] Mammalian orthologs and paralogs of yeast Atg8 play an essential role in the completion of autophagosome formation, and deficiency of their conjugation to lipids increases the number of unclosed autophagosomes in vivo.[6,7] Recent proteomic analyses, however, have revealed the existence of a number of LC3 (and other Atg8 orthologs)-binding proteins,[8] suggesting that LC3 plays additional roles in the regulation and modulation of autophagy.[9,10]

SQSTM1/p62 (sequestosome 1) is one of the best characterized LC3-binding proteins and is involved in selective autophagy, in which phagophores selectively recognize their substrates, e.g., protein aggregates and damaged organelles, for elimination.[10-12] In mammalian cells, polyubiquitination of the substrates triggers selective autophagy.[13,14] Because SQSTM1 contains both a ubiquitin-associated (UBA) domain, which recognizes polyubiquitin, and an LC3 recognition sequence (LRS) (also known as an LC3 interacting region [LIR] or Atg8-interacting motif [AIM]), which directly interacts with LC3, SQSTM1 has been proposed to act as a receptor protein that targets substrates to phagophores through direct interaction with substrate polyubiquitinated proteins and phagophore-associated LC3. However, the finding that core ATG proteins are recruited to the substrates of selective autophagy independently of LC3 suggests the presence of an unknown factor(s) that recognizes the substrates.[15-17] Because SQSTM1 itself is efficiently degraded by autophagy, degradation of SQSTM1 is often used as an index of autophagic activity.[18] Furthermore, recent studies have shown that SQSTM1 is recruited to an autophagosome formation site independently of its LC3-binding activity but that oligomerization activity through the N-terminal Phox and Bem1p (PB1) domain is required for the recruitment process.[19] Conversely, neither an oligomerization-deficient mutant nor an LC3-binding-deficient mutant of SQSTM1 was degraded by autophagy, indicating that the interaction between SQSTM1 and LC3 is required for efficient SQSTM1 degradation.[19]

We recently have identified TBC1D25/OATL1 as a novel LC3 homolog-binding protein.[20] TBC1D25 contains a TBC (Tre-2/Bub2/Cdc16)/RAB-GTPase-activating protein (GAP) domain[21] and functions as a GAP for RAB33B, which interacts with ATG16L1, an essential factor for autophagosome formation.[22] Although TBC1D25 also contains an LRS, which is necessary for recruitment of TBC1D25 to the phagophore membrane, in contrast to SQSTM1, TBC1D25 is not degraded by autophagy. However, the molecular mechanism by which TBC1D25 escapes autophagic degradation is unknown.

In this study we demonstrated that TBC1D25 possesses a PB1-like domain at its N terminus, indicating that TBC1D25 and SQSTM1 share the PB1(-like) domain and the LRS. The results of chimeric analyses between TBC1D25 and SQSTM1 and of the addition of artificial oligomerization ability to TBC1D25 indicated that oligomerized TBC1D25 mutants with the intact LRS are efficient substrates of autophagy. Based on our findings, we discuss the possible mechanism of TBC1D25 escape from autophagic degradation despite its presence at the phagophore.

Results

The LRS of TBC1D25 and SQSTM1 is necessary for autophagosomal localization, but not sufficient for autophagic degradation

Since both TBC1D25 and SQSTM1 contain the LRS, they were recruited to LC3-positive phagophores in mouse embryonic fibroblast (MEF) cells under starved conditions (Fig. 1B), a finding that was consistent with the results of previous studies.[10,19,20] Despite their localization at phagophores, only SQSTM1 was degraded by starvation, and its degradation was inhibited by the presence of the lysosomal protease inhibitors E64d and pepstatin A (Fig. 1C, lanes 1 to 3 in the middle panel). By contrast, no change in the level of TBC1D25 protein expression was observed under the same experimental conditions (Fig. 1C, lanes 1 to 3 in the top panel). The absence of TBC1D25 degradation activity in MEF cells is unlikely to be attributable to the presence of SQSTM1, a preferred autophagic substrate, because TBC1D25 was not degraded during starvation even in *sqstm1*-knockout (KO) MEF cells (Fig. 1C, lanes 4 to 6 in the top panel).

To determine the molecular basis for the differing susceptibility to autophagic degradation of TBC1D25 and SQSTM1, we first focused on the differences between the biochemical properties of their LRS. We have previously shown that the LRS of TBC1D25 interacts with GABARAP in vitro with greater affinity than it interacts with GABARAPL2/GATE-16 and LC3,[20] whereas the SQSTM1 LRS interacts with these 3 LC3 paralogs with almost similar affinity,[10] thereby raising the possibility that high affinity binding to GABARAP is involved in the escape of TBC1D25 from autophagic degradation. To pursue this possibility, we produced TBC1D25 and SQSTM1 LRS-swapping mutants, named TBC1D25-(SQT-LRS) and SQSTM1-(TBC-LRS) (Fig. 2A), and we produced WA mutants in which the Trp residue critical for LC3 homolog binding was mutated to Ala (Fig. 2A, shaded background), as a negative control (Fig. 2B, lanes 8, 11, and 14 in the top panel, and Fig. S1). As expected, TBC1D25-(SQT-LRS) exhibited reduced binding activity toward GABARAP and GABARAPL2 (Fig. 2B, compare lanes 10 and 12, and 13 and 15 in the top panel) without any change in its autophagosomal localization in MEF cells (Fig. S1B). However, the same as the wild-type TBC1D25, the TBC1D25-(SQT-LRS) was not degraded even under starved conditions (Fig. 2C, right panels). By contrast, both wild-type SQSTM1 and SQSTM1-(TBC-LRS) were present on LC3-positive autophagosomes (Fig. S1A) and degraded by starvation (Fig. 2C, left panels). These results indicated that the LRS of TBC1D25 and SQSTM1 is not a primary determinant of autophagic degradation of the LRS-containing proteins, although it is necessary for their autophagosomal localization.

Addition of the SQSTM1 PB1 domain to TBC1D25 is sufficient for it to undergo autophagic degradation

Although TBC1D25 was originally described as a protein that contains the TBC-RAB-GAP domain[20,23] and the LRS in the middle of the molecule but not any other protein motifs in its N or C terminus, close inspection of the N-terminal domain of TBC1D25 by means of the HHpred software program[24] indicated that it also contains a PB1-like domain that exhibits weak similarity to the N-terminal PB1 domain of SQSTM1 (Figs. 1A and S2). To determine whether the difference between the N-terminal PB1 domain of SQSTM1 and the PB1-like domain of TBC1D25 plays a role in the difference in the susceptibility of the proteins to undergo autophagic degradation, we next produced a series of chimeric mutants between TBC1D25 and SQSTM1 (summarized in Fig. 3) and investigated their subcellular
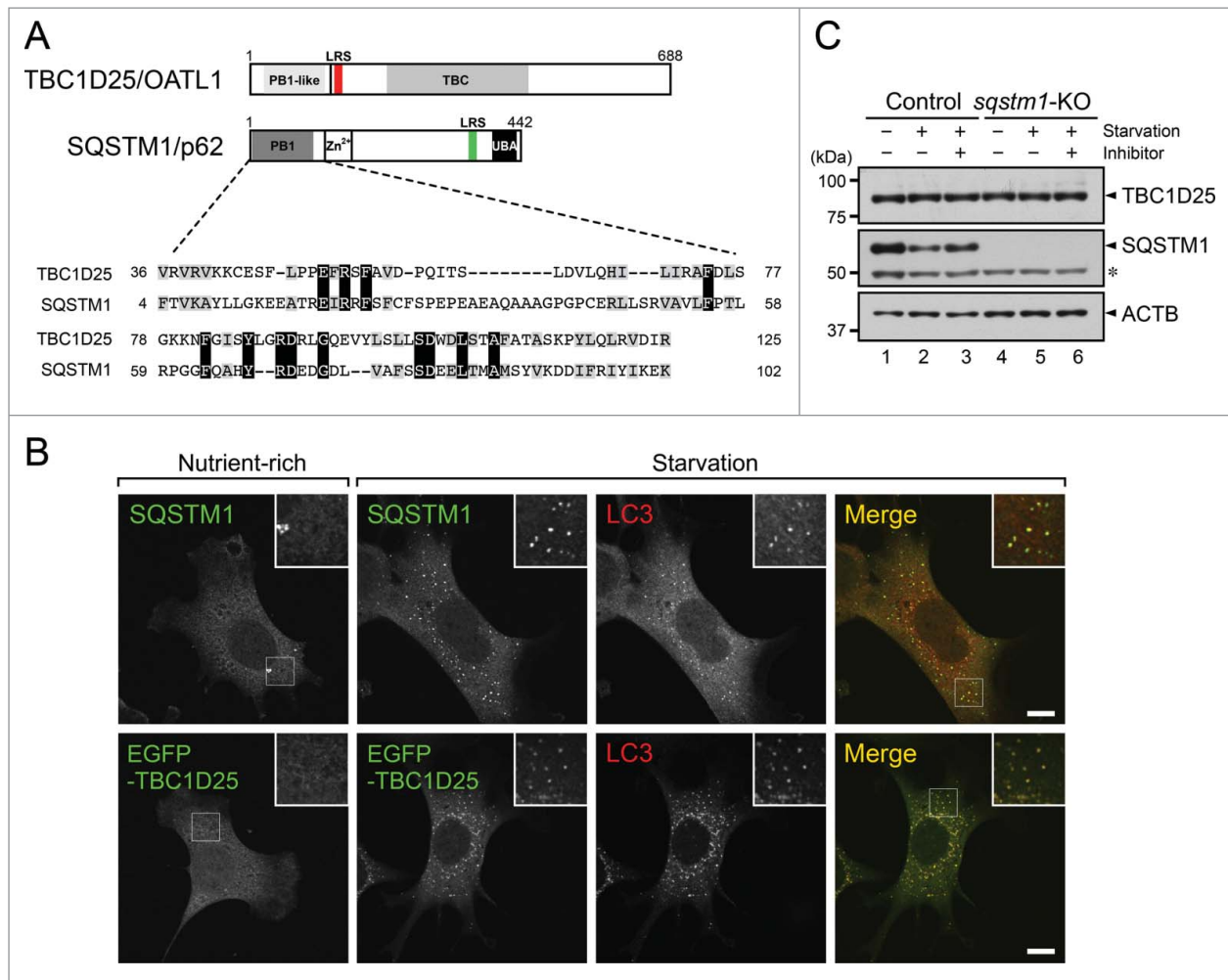
Figure 1. TBC1D25 is not a substrate of starvation-induced autophagy. (A) Domain organization of TBC1D25 and sequestosome-1 (SQSTM1) and sequence alignment of the PB1-like domain of TBC1D25 and PB1 domain of SQSTM1. The N-terminal domains of TBC1D25 and SQSTM1 were aligned by using the HHpred software program (see also Fig. S2). Amino acid residues in the sequences that are identical and similar are shown against a black background and a shaded background, respectively. (B) MEF cells stably expressing EGFP-TBC1D25 were cultured for 1 h under nutrient-rich conditions (far left column) or starved conditions (right 3 columns). Note that EGFP-TBC1D25 and endogenous SQSTM1 colocalized well with LC3 dots under starved conditions. Scale bars: 10 μm. (C) The TBC1D25 protein level in both control MEF cells and *sqstm1*-KO MEF cells was unaltered by starvation. Control MEF cells and *sqstm1*-KO MEF cells were cultured for 2 h in DMEM (nutrient-rich; - starvation) or HBSS (starvation) with or without 100 μM E64d and 100 μg/ml pepstatin A, and their cell lysates were analyzed by immunoblotting with anti-TBC1D25 antibody (top panel), anti-SQSTM1 antibody (middle panel), and anti-ACTB antibody (bottom panel). Note that SQSTM1, but not TBC1D25, was degraded by starvation. The asterisk indicates the nonspecific band of the anti-SQSTM1 antibody. The positions of the molecular mass markers (in kilodaltons) are shown on the left.

localization (Fig. 4) and whether they underwent starvation-induced degradation (Fig. 5). To do so, because SQSTM1 is known to form homo-oligomers,[10,19,25] we used *sqstm1*-KO MEF cells as a means of avoiding hetero-oligomerization between endogenous SQSTM1 and the exogenous chimeric mutants, which would probably trap the exogenous chimeric mutants in endogenous SQSTM1 protein aggregates. Consistent with the results obtained with the LRS-swapping mutants described above, the chimeric mutants, which contained an intact LRS, localized at LC3-positive autophagosomes irrespective of the presence of the N-terminal PB1 domain, whereas none of the mutants that lacked an intact LRS (i.e., WA mutation) formed any cytoplasmic dots at all (Fig. 4, 2, 4, 6, and 8 rows from the top). Intriguingly, PB1-TBC1D25ΔN, which contains the PB1 domain of SQSTM1, often formed cytoplasmic dots even under nutrient-rich conditions (Fig. 4, far left panel in the third row). More importantly, PB1-TBC1D25ΔN underwent starvation-induced degradation, the same as SQSTM1 did (compare lanes 1 and 2, and lanes 9 and 10 in Fig. 5A and 5B), and the WA mutation completely abrogated their degradation (compare lanes 3 and 4, and lanes 11 and 12 in Fig. 5A and 5B). Moreover, starvation-induced degradation of PB1-TBC1D25ΔN was inhibited by the presence of BafA1 (Fig. S3A), the same as starvation-induced degradation of SQSTM1 was, indicating that PB1-TBC1D25ΔN is likely to be degraded by autophagy. By contrast, the same as the wild-type TBC1D25 (Fig. 1C), neither TBC1D25ΔN nor the TBC1D25ΔN-WA underwent starvation-induced degradation (lanes 5 to 8 in Fig. 5A and 5B).

Because the UBA domain of SQSTM1 has also been suggested to be involved in autophagic degradation of SQSTM1,[10,25] we produced 4 additional TBC1D25 mutants with the UBA domain of SQSTM1 at the C terminus (Fig. 3). However, the C-terminal addition of the UBA domain to TBC1D25 did not appear to alter the properties
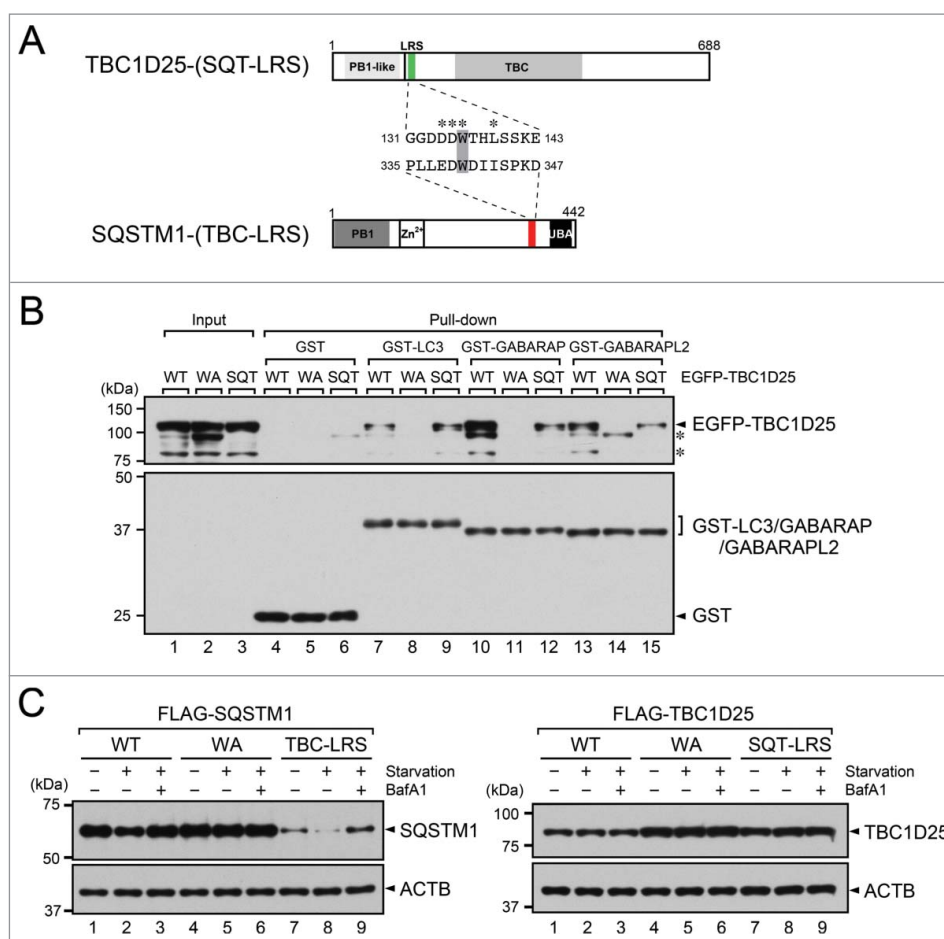
Figure 2. The LRS of SQSTM1 and TBC1D25 is essential for phagophore localization, but not sufficient for their degradation. (A) Schematic representation of the LRS-swapping mutants of TBC1D25 and SQSTM1, named TBC1D25-(SQT-LRS) and SQSTM1-(TBC-LRS), respectively. The asterisks indicate the residues that are highly conserved in many LRSs. The WA mutant contains a Trp-to-Ala (WA) mutation (shaded background), which disrupts binding activity to LC3 homologs. (B) Differing LC3 homolog binding activity of TBC1D25, TBC1D25-W136A (designated as WA), and TBC1D25-(SQT-LRS) (designated as SQT) as revealed by GST affinity isolation assays. COS-7 cell lysates expressing EGFP-TBC1D25, EGFP-TBC1D25-WA, or EGFP-TBC1D25-(SQT-LRS) were incubated with GST-LC3, GST-GABARAP, or GST-GABARAPL2 that had been coupled with glutathione-Sepharose beads. Proteins bound to the beads were analyzed by immunoblotting with HRP-conjugated anti-GFP antibody (top panel) and HRP-conjugated anti-GST antibody (bottom panel). The asterisks indicate the nonspecific bands of the anti-GFP antibody. (C) *sqstm1*-KO MEF cells stably expressing FLAG-SQSTM1, FLAG-SQSTM1-WA, FLAG-SQSTM1-(TBC-LRS) (FLAG-SQSTM1; left panels), FLAG-TBC1D25, FLAG-TBC1D25-WA, or FLAG-TBC1D25-(SQT-LRS) (FLAG-TBC1D25; right panels) were cultured for 2 h in DMEM (nutrient-rich; - starvation) or HBSS (starvation) with or without 20 μM BafA1. Cell lysates were analyzed by immunoblotting with anti-FLAG tag antibody (top panels) and anti-ACTB antibody (bottom panels). The positions of the molecular mass markers (in kilodaltons) are shown on the left.

of TBC1D25ΔN at all: the mutant proteins were recruited to LC3-positive phagophores in an LRS-dependent manner irrespective of the presence of the UBA domain (Fig. 4, bottom 4 rows) and only PB1-TBC1D25ΔN-UBA was degraded during starvation (lanes 17 and 18 in Fig. 5A and 5B). The above results taken together indicated that the PB1 domain of SQSTM1 is required for its autophagic degradation and that addition of the SQSTM1 PB1 domain to the LRS-containing protein TBC1D25 is sufficient for it to undergo autophagic degradation.

Conferring artificial oligomerization ability on TBC1D25 enables autophagic degradation of the mutant TBC1D25

Because the PB1 domain of SQSTM1 possesses self-oligomerization activity and because the results of coimmunoprecipitation assays showed that PB1-TBC1D25ΔN, but not TBC1D25 itself, is able to form a homo-oligomer (Fig. 6),[10,19] we attempted to determine whether oligomerization of LRS-

containing proteins is a key determinant of their autophagic degradation. To do so, we turned our attention to an artificial oligomerization tool, i.e., a mutant FKBP1A/FKBP12 (FK506 binding protein 1A) that contains a Phe-to-Met substitution at amino acid position 37 (referred to as FM below) (Fig. S4A).[26] We used the FM domain to prepare 3 tags having different oligomerization activity, i.e., tags FM1, FM2, and FM4 (see Fig. 7A for details). In brief, FM2 and FM4 consist of 2 FMs in tandem and 4 FMs in sequence, respectively. Another important merit of the FM tags is that their artificial oligomerization activity can be regulated in living cells by using the D/D solubilizer,[26] a synthetic derivative of rapamycin that rapidly disrupts oligomerization of the FM domains. When EGFP-tagged FM1, FM2, and FM4 were each expressed alone in MEF cells, most of all 3 FM proteins was mostly present in the cytosol, although several dots were observed in some cells expressing EGFP-FM4 (Fig. S4C). These FM proteins are unlikely to be substrates of autophagy, because their protein expression level was unaltered by starvation (Fig. S4B) and they hardly colocalized with LC3
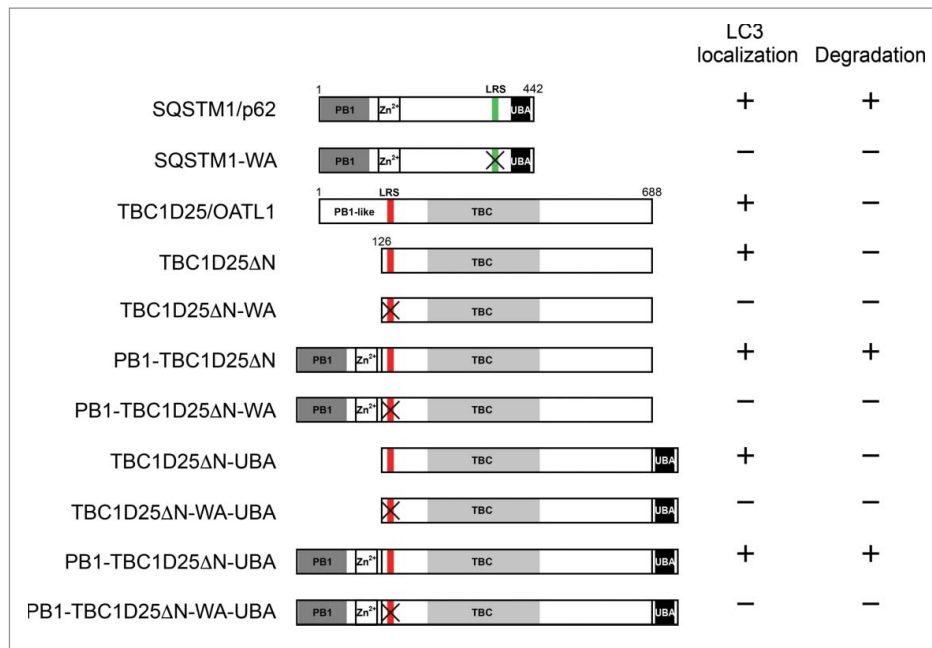
Figure 3. Schematic representation of the TBC1D25-chimera mutants with SQSTM1, named TBC1D25ΔN, TBC1D25ΔN-WA, PB1-TBC1D25ΔN, PB1-TBC1D25ΔN-WA, TBC1D25ΔN-UBA, TBC1D25ΔN-WA-UBA, PB1-TBC1D25ΔN-UBA, and PB1-TBC1D25ΔN-WA-UBA. Colocalization with LC3 (see Figs. 4 and S1) and degradation susceptibility (see Fig. 5) of the TBC1D25-chimera mutants under starved conditions are shown at the right of each construct. The WA mutants that lack an LRS (indicated by the black cross representing LRS being crossed out) are unable to target LC3-positive phagophores (see Figs. 4 and S1).

(Fig. S4C, far right panels). We therefore concluded that the FM-tags are ideal tools for conferring distinct oligomerization ability on TBC1D25 and prepared 3 FM-tagged TBC1D25 mutants: FM1-TBC1D25ΔN, FM2-TBC1D25ΔN, and FM4-TBC1D25ΔN (Fig. 7A).

When the FM-tagged TBC1D25 mutants were expressed in MEF cells, in contrast to the EGFP-fused FM-tags alone (Fig. S4C), all of the mutants were recruited to LC3-positive phagophores (Fig. 8). It should be noted that the (LC3)-FM4-TBC1D25ΔN double-positive dots were clearly larger in size than the (LC3)-FM1-TBC1D25ΔN and (LC3)-FM2-TBC1D25ΔN double-positive dots (Fig. 8, insets in the top 3 rows), suggesting that the existence of a positive correlation between oligomerization activity and autophagosome size. We next assessed starvation-induced degradation of FM-tagged TBC1D25ΔN mutants (Fig. 7B and 7C). Intriguingly, both FM2-TBC1D25ΔN and FM4-TBC1D25ΔN, but not FM1-TBC1D25ΔN, underwent starvation-induced degradation, the same as SQSTM1 did (Fig. 7B, compare lanes 4 and 5, 7 and 8, and 10 and 11). To determine whether the oligomerization activity of FM2 and FM4 was directly involved in the autophagic degradation of FM2-TBC1D25ΔN and FM4-TBC1D25ΔN, we treated the cells with the D/D solubilizer. As expected, the D/D solubilizer decreased the size of the (LC3)-FM4-TBC1D25ΔN double-positive dots to the size of the (LC3)-FM1-TBC1D25ΔN double-positive dots (Fig. 8, insets in the bottom 3 rows) and inhibited starvation-induced degradation of FM2-TBC1D25ΔN and FM4-TBC1D25ΔN (Fig. 7C). These effects of the D/D solubilizer are unlikely to be caused by inhibition of starvation-induced autophagy itself, because the D/D solubilizer had no significant effect on the formation of LC3 dots (Fig. S5) or degradation of SQSTM1 (Fig. 7B, compare lanes 2 and 3 in the top panel).

TBC1D25 is specifically localized at the outer autophagosomal membrane

Finally, we investigated whether TBC1D25 is localized inside, outside, or both inside and outside autophagosomes in MEF cells at the electron microscopy level. As shown in Fig. 9 (top 2 rows), EGFP-tagged LC3, a phagophore-associated binding partner of TBC1D25, was nearly equally localized at the inner membrane and outer membrane of the autophagosome (red arrowheads; $58.8 \pm 5.2\%$ of LC3 dots at the outer membrane; n = 13 profiles). The EGFP-tagged TBC1D25, however, was mostly localized at the outer autophagosomal membrane (red arrowheads; $93.4 \pm 3.3\%$ of TBC1D25 dots at the outer membrane; n = 9 profiles). By contrast, 2 other oligomerized LC3-binding proteins, EGFP-tagged SQSTM1 and PB1-TBC1D25ΔN, were distributed at both the inner membrane and outer membrane of autophagosomes, the same as EGFP-tagged LC3 was: $31.4 \pm 9.9\%$ (n = 10 profiles) of the EGFP-tagged SQSTM1 dots and $41.9 \pm 6.5\%$ (n = 13 profiles) of the EGFP-tagged PB1-TBC1D25ΔN dots were found at the outer membrane (Fig. 9, bottom 2 rows). These results indicate that the asymmetrical localization of TBC1D25 on the autophagosome is likely to ensure escape of TBC1D25 from autophagic degradation.

Discussion

LC3 is the best characterized mammalian ortholog family of yeast Atg8[4] and is thought to be involved in the autophagosome closure step.[6,7] LC3 is localized both inside and outside the autophagosome and binds to a variety of molecules, including SQSTM1, a receptor protein between phagophore-associated LC3 and polyubiquitinated substrate proteins.[8,9] Although
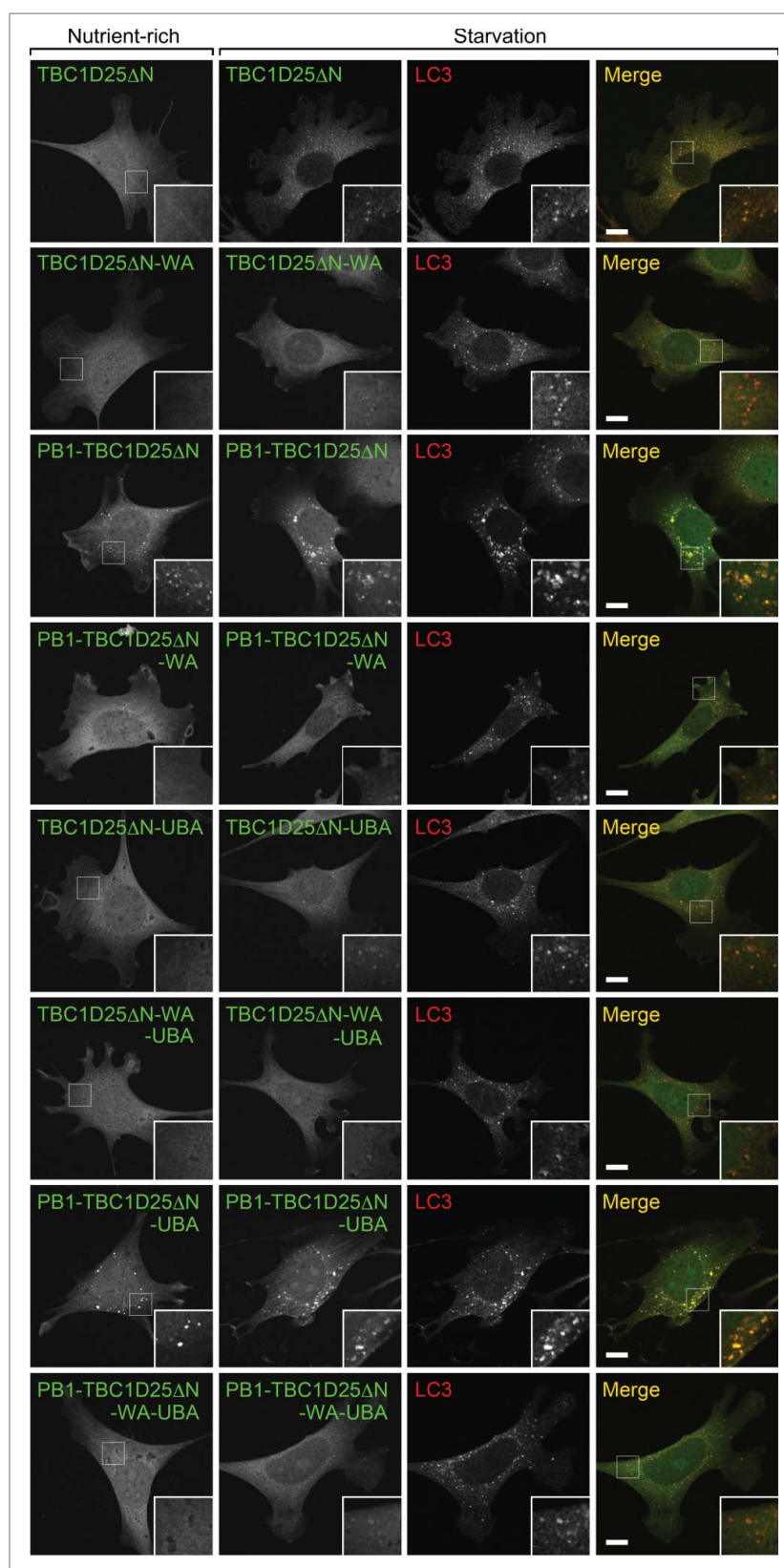
Figure 4. Colocalization of TBC1D25-chimera mutants with LC3. *sqstm1*-KO MEF cells stably expressing EGFP-TBC1D25ΔN, EGFP-TBC1D25ΔN-WA, EGFP-PB1-TBC1D25ΔN, EGFP-PB1-TBC1D25ΔN-WA, EGFP-TBC1D25ΔN-UBA, EGFP-TBC1D25ΔN-WA-UBA, EGFP-PB1-TBC1D25ΔN-UBA, or EGFP-PB1-TBC1D25ΔN-WA-UBA were cultured for 1 h in DMEM (nutrient-rich; far left column) or HBSS (starvation; right 3 columns). Note that cytoplasmic dots were often observed in the cells expressing an TBC1D25 mutant with the LRS that contained a PB1 domain, i.e., EGFP-PB1-TBC1D25ΔN and EGFP-PB1-TBC1D25ΔN-UBA, even under nutrient-rich conditions, whereas no dots were observed with other TBC1D25 mutants under nutrient-rich conditions. Scale bars: 10 μm.
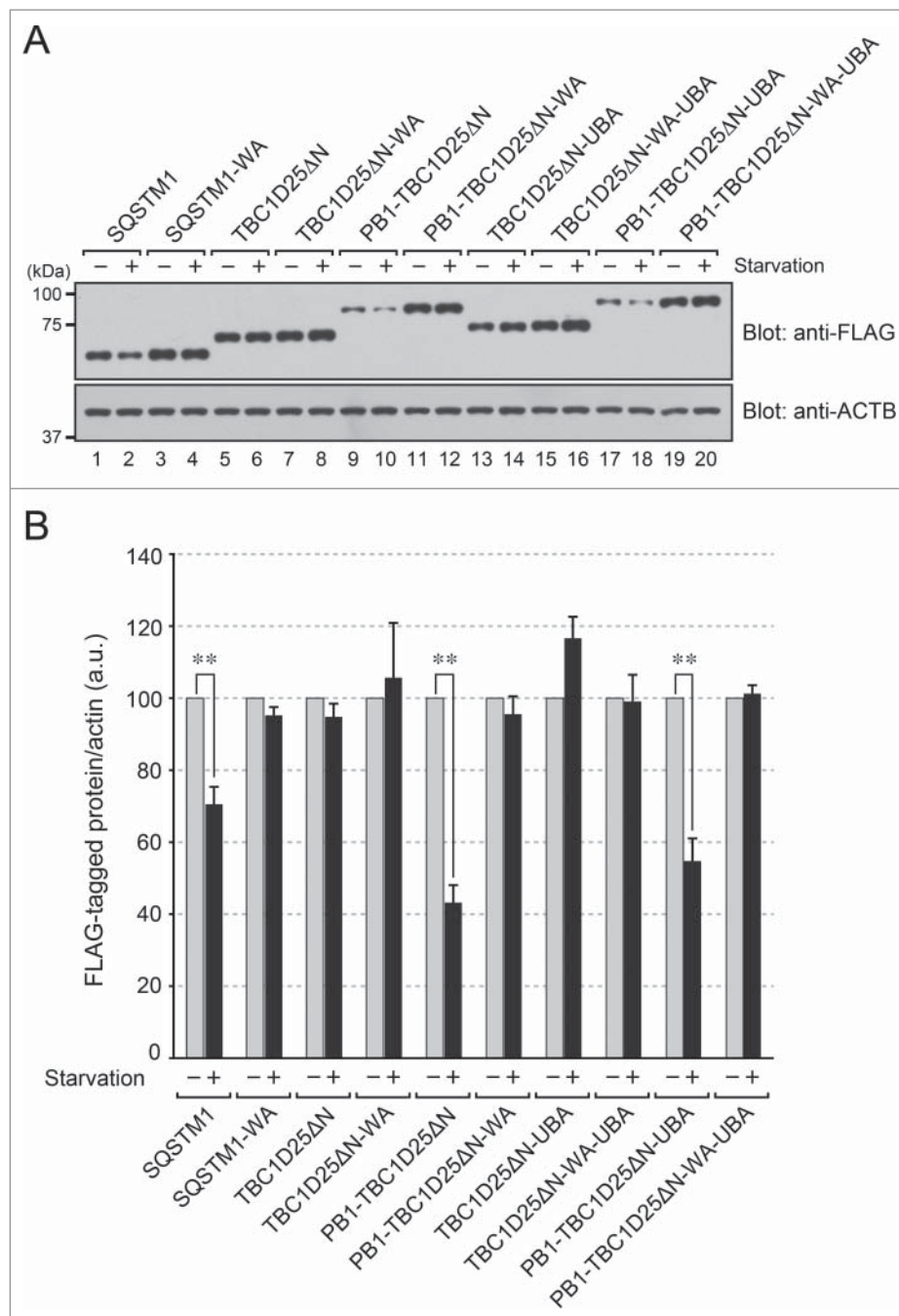
Figure 5. The PB1 domain of SQSTM1 is necessary for starvation-induced degradation of TBC1D25-chimera mutants. (A) *sqstm1*-KO MEF cells stably expressing the indicated FLAG-tagged SQSTM1 (wild-type and WA) and TBC1D25 chimera mutants were cultured for 2 h in DMEM (nutrient-rich; - starvation) or HBSS (starvation). Cell lysates were analyzed by immunoblotting with anti-FLAG tag antibody (top panel) and anti-ACTB antibody (bottom panel). The levels of PB1-TBC1D25ΔN expression (lanes 9 and 10) and PB1-TBC1D25ΔN-UBA expression (lanes 17 and 18) were much lower than the levels of expression of other TBC1D25 mutants, because both of these proteins were degraded by basal autophagy even under nutrient-rich conditions (see Fig. S3B). (B) Quantification of the band intensity of FLAG-tagged proteins shown in the top panel in **A**. The bars represent the means and SE of data from 3 independent experiments. **, $P < 0.01$ (The Student unpaired t test). a.u., arbitrary units.

SQSTM1 itself is degraded by autophagy, the same as autophagic substrates, whether or not other LC3-binding proteins are also degraded by autophagy largely remains to be determined. In the present study we compared the susceptibility of SQSTM1 and a RAB33B-GAP TBC1D25 to autophagic degradation and confirmed that TBC1D25 is not a substrate of autophagy (Fig. 1C)[20] despite containing the N-terminal PB1-like domain and LRS, the same as SQSTM1 does (Fig. 1A). We demonstrated by chimeric analysis between TBC1D25 and SQSTM1 that the difference between the properties of the PB1-like

domain of TBC1D25 and the PB1 domain of SQSTM1 determines their fate in regard to autophagic degradation (Figs. 3 to 5). By contrast, the LRS of both TBC1D25 and SQSTM1 is a prerequisite for their phagophore localization, but it is not a primary determinant of their autophagic degradation (Fig. 2).

The PB1 domain is a protein interaction module that is conserved in a variety of species, including fungi, plants, and animals, and it often forms a PB1 to PB1 heterodimer.[27] Based on their sequences, PB1 domains are classified into 3 types (type I, type II, and type I/II); type I PB1 domains (e.g., NBR1 and
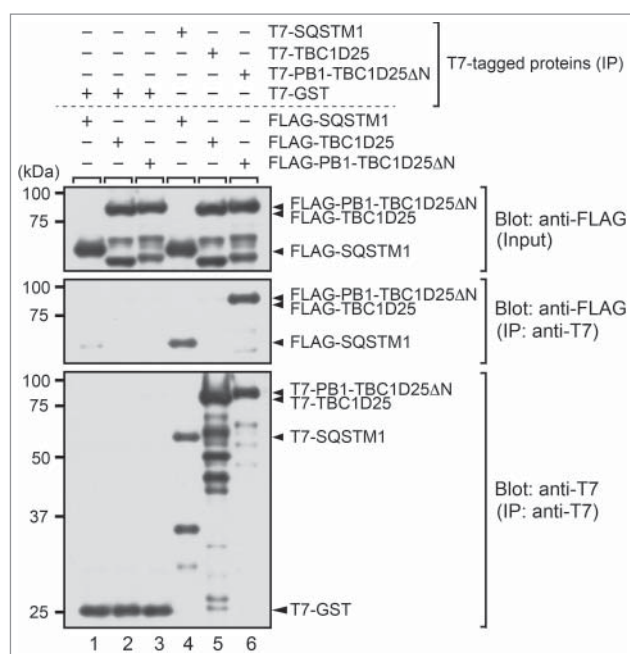
Figure 6. Differing oligomerization activity of TBC1D25, PB1-TBC1D25ΔN, and SQSTM1. COS-7 cells transiently expressing T7-tagged TBC1D25, PB1-TBC1D25ΔN, SQSTM1, or GST, or FLAG-tagged TBC1D25, PB1-TBC1D25ΔN, or SQSTM1 were harvested and lysed. Association between T7-tagged and FLAG-tagged proteins was evaluated by coimmunoprecipitation assays using agarose beads coupled with anti-T7 tag antibody followed by immunoblotting with the antibodies indicated as described previously.[39] T7-GST was used as a negative control (lanes 1 to 3). Input means 1/200 volume of the reaction mixture. The positions of the molecular mass markers (in kilodaltons) are shown on the left.

NCF4/p40^{phox}) contain an acidic OPCA motif, whereas type II PB1 domains (e.g., PARD6A/PAR6A and NCF2/p67^{phox}) contain the invariant Lys residue on the first β strand, and type I/II PB1 domains (e.g., SQSTM1) contain both (Fig. S2).[27] In contrast to the canonical PB1 domain, however, the PB1-like domain of TBC1D25 lacks a conserved Lys residue and acidic residues (Fig. S2), both of which are involved in the PB1-PB1 interaction, suggesting that the PB1-like domain of TBC1D25 is unlikely to mediate strong PB1-PB1 interactions. Actually, the homo-oligomerization activity of TBC1D25 appeared to be weaker than that of PB1-TBC1D25ΔN and SQSTM1 (Fig. 6). Moreover, addition of the SQSTM1 PB1 domain or FM2/4, i.e., artificial oligomerization domains, to the N terminus of TBC1D25ΔN was sufficient to enable autophagic degradation of the fusion proteins (Figs. 5 and 7), whereas addition of FM1, which mediates dimer formation alone, to the N terminus in TBC1D25ΔN was not. The above results taken together indicated that the difference between the oligomerization activity of the N-terminal domains of TBC1D25 and SQSTM1 is likely to determine their fate, i.e., escape from the autophagosome and autophagic degradation, respectively. Although the PB1-like domain of TBC1D25 does not serve as an oligomerization site, it is still possible that the PB1-like domain regulates autophagy by binding other molecules. Future identification of the PB1-like domain-binding partner would clarify the function of this domain during autophagy, especially at the autophagosome maturation step.[20]

What mechanism is responsible for the less-oligomerized LRS-containing TBC1D25 being excluded from inside the

autophagosome (Fig. 9)? It has recently been reported that SQSTM1 is recruited to the autophagosome formation site independently of the LRS and that the oligomerization activity of SQSTM1 is required for this recruitment process.[19] We assume that oligomerized PB1-TBC1D25ΔN and FM2/4-TBC1D25ΔN are also recruited to the autophagosome formation site by unknown mechanisms. Consistent with our assumption, both PB1-TBC1D25ΔN and FM2/4-TBC1D25ΔN were clearly present at ULK1-positive dots in wortmannin-treated cells, the same as SQSTM1 was (Fig. S6, 3 left panels in 3, 5, and 6 rows), whereas the D/D solubilizer treatment resulted in the disappearance of FM2/4-TBC1D25ΔN signals from the ULK1-positive dots (Fig. S6, 3 right panels in the bottom 2 rows). In other words, the less-oligomerized TBC1D25 is unable to access the autophagosome formation site, because the inner space of the autophagosome is already occupied by oligomerized LRS-containing proteins, e.g., SQSTM1. Although TBC1D25 is not degraded during starvation even in *sqstm1*-KO MEF cells (Fig. 1C, lanes 4 to 6 in the top panel), we speculate that other LRS-containing proteins, e.g., NBR1 and NCOA4, which is involved in autophagic degradation of ferritin,[28,29] are still present at the autophagosome formation site and contribute to excluding TBC1D25 from inside the autophagosome. Alternatively, the asymmetric outer membrane localization of TBC1D25 may occur independently of protein clusters inside the autophagosome, because the availability of TBC1D25 between inside and outside the autophagosome appears to differ, i.e., cytoplasmic TBC1D25 is freely recruited to LC3 on the outer membrane, whereas its access to the inner membrane may be restricted by the elongating phagophore, and the amount of TBC1D25 trapped inside the autophagosome may be much smaller than the amounts of oligomerized LRS-containing proteins.

We noted 2 recent studies of TBC1D5 and FYCO1, both of which contain an LRS and localize at phagophores[30,31] (reviewed in ref. 32). TBC1D5, another RAB-GAP, is not an autophagic substrate despite interacting with LC3 and is involved in endocytosis and autophagy.[30] FYCO1 is specifically localized outside the autophagosome and is involved in autophagosome transport through interaction with LC3 and kinesin.[31] Although it remains to be determined whether TBC1D5 exhibits asymmetric autophagosomal localization and whether FYCO1 is not an autophagic substrate, it is tempting to speculate that both of these LRS-containing proteins have a less-oligomerized nature similar to that of TBC1D25. Actually, we found that TBC1D5 and another LC3-binding protein TBC1D2B[20] do not form an oligomer (Fig. S7A and S7C) and that both TBC1D2B and TBC1D5 do not undergo starvation-induced autophagic degradation (Fig. S7D), even though they clearly colocalize with LC3 dots (Fig. S7B). More importantly, addition of the PB1 domain to the N terminus of these 2 proteins caused their autophagic degradation (Fig. S7D). We thus assume that the asymmetric localization of less-oligomerized LRS-containing proteins outside the autophagosome ensures efficient transport and maturation of the autophagosome. We also noted a previous study of NBR1, which can form a hetero-oligomer with other PB1-containing proteins, including
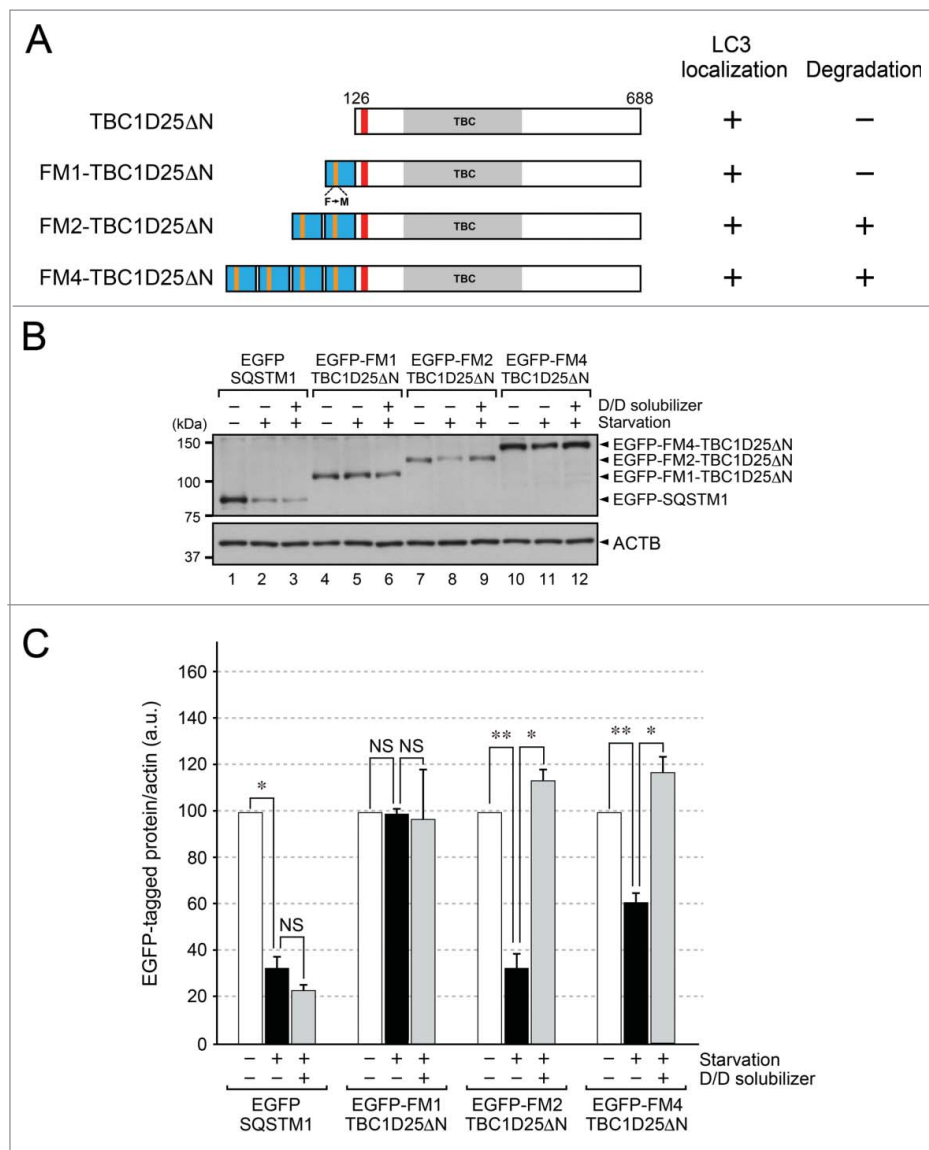
Figure 7. Addition of the artificial oligomerization domains (FM2 and FM4) to the N terminus of TBC1D25 resulted in starvation-induced degradation of the mutant proteins. (A) Schematic representation of the TBC1D25ΔN mutants with FKBP-FM domains, which are known to be artificial oligomerization tools.[26] One FKBP-FM domain, tandem FKBP-FM domains (named FM2), and 4 FKBP-FM domains (named FM4) were added to the N-terminal domain of TBC1D25ΔN (referred to as FM1-TBC1D25ΔN, FM2-TBC1D25ΔN, and FM4-TBC1D25ΔN, respectively). Colocalization with LC3 (Fig. 8) and degradation susceptibility (in C) of the EGFP-tagged FM-fusion proteins under starved conditions are shown at the right of each construct. (B) FM2-TBC1D25ΔN and FM4-TBC1D25ΔN undergo starvation-induced degradation in an oligomerization-dependent manner. *sqstm1*-KO MEF cells stably expressing EGFP-tagged SQSTM1 or FM1/2/4-TBC1D25ΔN mutants were cultured for 6 h in DMEM (nutrient-rich; - starvation) or HBSS (starvation) with or without 1 μM D/D solubilizer. Cell lysates were analyzed by immunoblotting with anti-GFP antibody (top panel) and anti-ACTB antibody (bottom panel). The positions of the molecular mass markers (in kilodaltons) are shown on the left. (C) Quantification of the band intensity of EGFP-tagged proteins shown in the top panel in (B). The bars represent the means and SE of data from 3 independent experiments. *, $P < 0.05$ **; $P < 0.01$ (Dunnett test). NS, not significant.

SQSTM1, and is degraded by starvation-induced autophagy, the same as SQSTM1,[33] supporting our hypothesis that oligomerized LC3-binding proteins are substrates of autophagy.

In summary, we have investigated the differing susceptibility to autophagic degradation of 2 LRS-containing proteins, TBC1D25 and SQSTM1, in MEF cells and demonstrated that the difference in their oligomerization activity is the primary reason why the less-oligomerized TBC1D25 is not degraded by starvation-induced autophagy. Our findings suggest that oligomerization can serve as a new indicator of the susceptibility of LC3-binding proteins to autophagic degradation. It will be interesting to investigate the relationship between the oligomerization activity and susceptibility to

autophagic degradation of other LC3-binding proteins to determine whether or not oligomerized LRS-containing proteins are efficient substrates of autophagy.

Materials and methods

Antibodies and reagents

Anti-LC3 rabbit polyclonal antibody and anti-TBC1D25 rabbit polyclonal antibody were affinity-purified as described previously.[20,22,34] Horseradish peroxidase (HRP)-conjugated anti-FLAG tag (M2) mouse monoclonal antibody (Sigma-Aldrich, A8592), anti-GFP polyclonal antibody
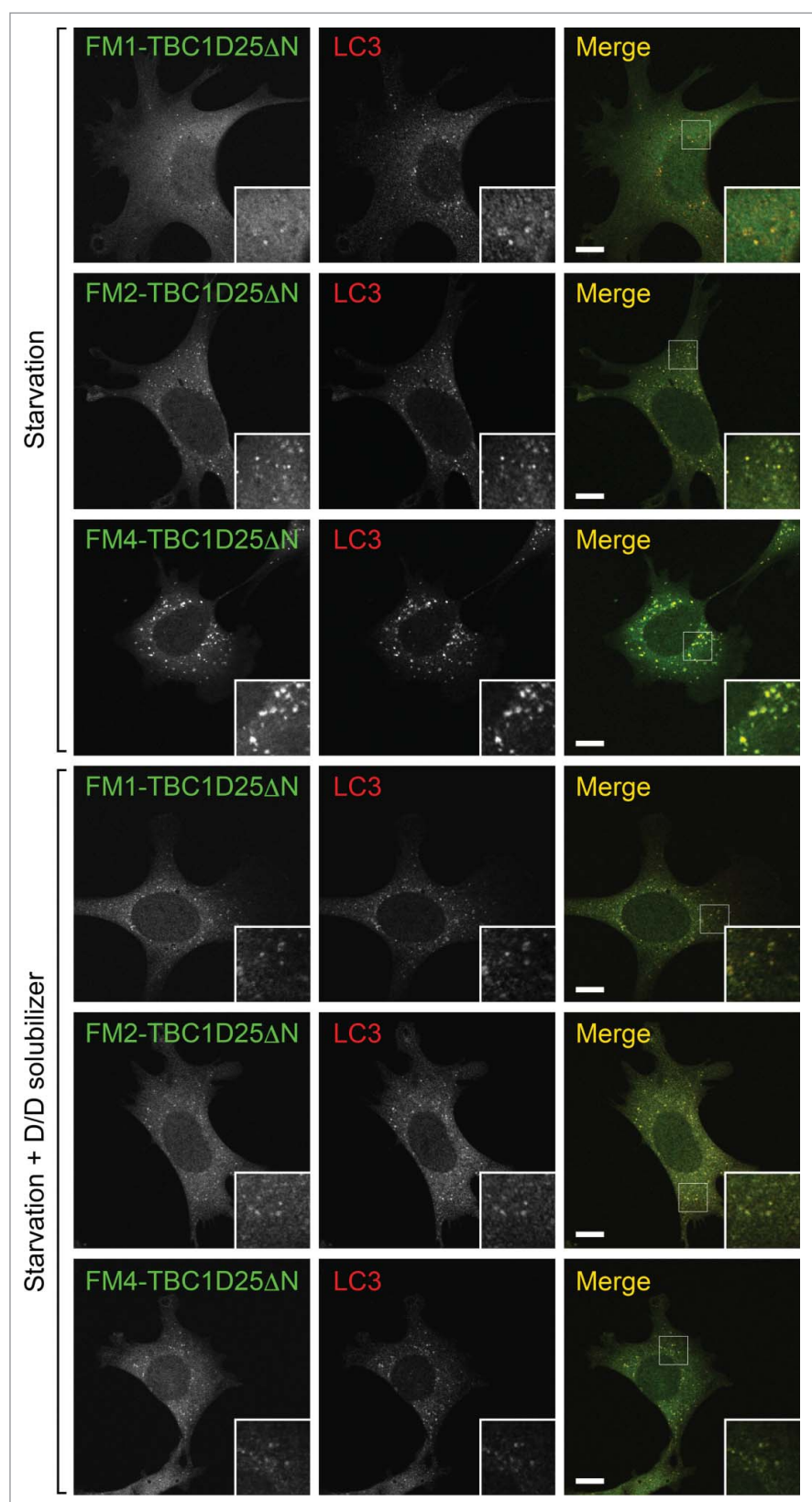
Figure 8. Colocalization of FM-fusion proteins of TBC1D25ΔN mutants with LC3. *sqstm1*-KO MEF cells stably expressing EGFP-tagged SQSTM1, FM1-TBC1D25ΔN, FM2-TBC1D25ΔN, or FM4-TBC1D25ΔN were cultured for 1 h in HBSS (starved conditions) with (monomer conditions) or without 1 μM D/D solubilizer (oligomerization conditions). Note that all of the FM-fusion proteins colocalized well with LC3 dots under starved conditions irrespective of the presence of the D/D solubilizer. Scale bars: 10 μm.
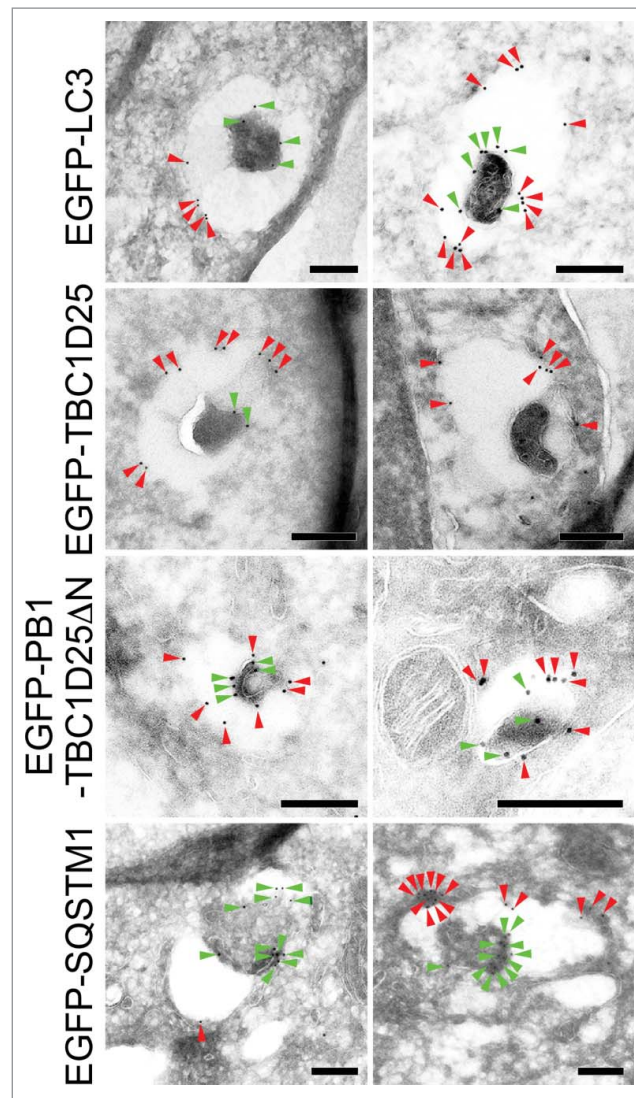
Figure 9. Asymmetric localization of TBC1D25 on autophagosomes. MEF cells stably expressing EGFP-tagged LC3, TBC1D25, PB1-TBC1D25ΔN, or SQSTM1 were analyzed by ultrathin cryosection immunoelectron microscopy using anti-GFP antibody and a secondary antibody conjugated with colloidal gold particles (12 nm). Green arrowheads and red arrowheads indicate gold particles on inner membranes and outer membranes, respectively, of the autophagosome. Note that TBC1D25 was mainly localized outside the autophagosome, whereas the other 3 proteins were rather uniformly localized inside and outside the autophagosome. Scale bars: 200 nm.

(MBL, 598), anti-ACTB/β-actin mouse monoclonal antibody (Applied Biological Materials, G043), HRP-conjugated anti-GST antibody (Santa Cruz Biotechnology, Inc., sc-459), HRP-conjugated anti-T7 tag mouse monoclonal antibody (Merck Millipore, 69048), anti-T7 tag mouse monoclonal antibody-conjugated agarose (Merck Millipore, 69026), anti-HA tag mouse monoclonal antibody (12CA5; Roche Life Science, 11583816001), anti-SQSTM1/p62 rabbit polyclonal antibody (Enzo life Sciences, Inc., PW9860-0100), and Alexa Fluor 594-conjugated secondary antibodies (Invitrogen, A-11012) were obtained commercially. Glutathione-Sepharose 4B was purchased from GE Healthcare (17-0756-05). E64d and pepstatin A were purchased from Peptide Institute, Inc. (4321-v and 4397-v, respectively). D/D solubilizer, Bafilomycin A$_1$ (BafA1), and wortmannin were from Takara Bio Inc. (635054), Merck Millipore (196000-10UGCN), and Merck Biosciences Calbiochem (681676), respectively.

Cell culture

Wild-type and *sqstm1/p62*-KO MEF cells were a kind gift from Noboru Mizushima (University of Tokyo, Tokyo, Japan) and Masaaki Komatsu (Niigata University, Niigata, Japan), respectively.[35] Plat-E cells were donated by Toshio Kitamura (University of Tokyo, Tokyo, Japan). MEF cells and COS-7 cells were maintained at 37°C in DMEM (Wako Pure Chemical Industries, Ltd., 044-29765) containing 10% fetal bovine serum and the antibiotics streptomycin and penicillin-G under a 5% CO$_2$ atmosphere. To achieve starvation, MEF cells were washed once with HBSS (Sigma-Aldrich, H9269) and transferred to HBSS. Plat-E cell culture and retrovirus infection were performed essentially as described previously.[36] Lysosomal proteases were inhibited by exposing cells for 2 h to either 20 nM BafA1 or 100 nM E64d and 100 μg/ml pepstatin A under starved conditions. Artificially oligomerized FM fusion proteins

were dissociated by exposing MEF cells to 1 μM D/D solubil-izer for 1 h (Figs. 8 and S5) or 6 h (Fig. 7).

Plasmid construction

pEGFP-C1-TBC1D25, pEGFP-C1-TBC1D25[W136A] (TBC1D25-WA), pEF-T7-GST-LC3B (LC3), pEF-T7-GST-GABARAP and pEF-T7-GST-GABARAPL2/GATE-16 were prepared as described previously.[20,22] The cDNA encoding mouse *Sqstm1* was amplified from Marathon-Ready adult mouse brain cDNA (BD Biosciences Clontech, 639400) by using conventional PCR techniques and the following pair of oligonucleotides with a BamHI linker (underlined) or a stop codon (bold face): 5′-GGATCCATGGCGTCGTTCACGGTGAAGGCC-3′ and 5′-**TCA**CAATGGTGGAGGGTGCTTCGAATACT-3′. A mutant cDNA fragment encoding an LRS-swapping *Tbc1d25* mutant, named *Tbc1d25*-(SQT-LRS), was obtained by using the PCR sewing methods,[37] and KOD plus ver. 2 (Toyobo Co., Ltd., KOD-211), as well as the pEGFP-C1-TBC1D25 plasmid were used as the polymerase for PCR and as the template, respectively. The following primers were used for amplification: 5′-ACGATGACTGGACACATTTGTCTTCAAAAGAAG TCATTGGCTCCGACGTG-3′ and 5′-GAAGACAAATGTGT CCAGTCATCGTCTCCTCCGCTGTCCTCCGAGGGCCG-3′. Deletion mutants of *Tbc1d25* and *Sqstm1* and their chimeric mutants were constructed by using conventional PCR techniques and KOD plus ver. 2. The following pairs of oligonucleotides with a restriction enzyme site (underlined) or a stop codon (bold face) were used for amplification: 5′-AGATCTCCCTCGGAGGACAGCCCATT-3′ and 5′-**TCA**A-GATGCGGCTGTGGC-3′ for *Tbc1d25*ΔN; 5′-AGATCTCCCT CGGAGGACAGCCCATT-3′ and 5′-GTCGACGATGCGGCT GTGGCC-3′ for *Tbc1d25*ΔN (without a stop codon); 5′-GTCGACAGAGGCTGATCCCCGG-3′ and 5′-**TCA**-CAATGGTGGAGGGTGCTTCGAATACT-3′ for *Sqstm1*-UBA; and 5′-GGATCCATGGCGTCGTTCACGGTGAAGGC C-3′ and 5′-AGATCTGTTGGGAAAGATGAGCTTGCT-3′ for *Sqstm1*-PB1. The *Tbc1d25*ΔN or *Tbc1d25*ΔN-WA cDNA fragment obtained with or without *Sqstm1*-PB1 and/or *Sqstm1*-UBA were inserted into the pMRX-IRES-puro/bsr-EGFP/FLAG vector, variants of pMRX-IRES-puro/bsr (donated by Shoji Yamashita, Tokyo Medical and Dental University, Tokyo, Japan)[38] and/or into the pEF-FLAG/T7 tag expression vector[39] by the standard molecular biology techniques. The resulting plasmids were referred to as pMRX-IRES-puro/bsr-EGFP/FLAG-TBC1D25ΔN, -TBC1D25ΔN-WA, -PB1-TBC1D25ΔN, -PB1-TBC1D25ΔN-WA, -TBC1D25ΔN-UBA, -TBC1D25ΔN-WA-UBA, -PB1-TBC1D25ΔN-UBA, and -PB1-TBC1D25ΔN-WA-UBA (see Fig. 3 for details). SQSTM1-WA and SQSTM1-(TBC-LRS) mutants were similarly produced by the PCR sewing methods described above by using the following pairs of oligonucleotides: 5′-GACGAT-GACGCGACACATTT-3′ and 5′-AAATGTGTCGCGT-CATCGTC-3′ for *Sqstm1*-W340A (*Sqstm1*-WA); and 5′-GAAGACTGGGACATAATCAGCCCCAAAGATGTGGACC CATCTACAGGT-3′ and 5′-GCTGATTATGTCCCAGTCTT CTAGCAATGGTGAGCAGTTTCCCGACTC-3′ for *Sqstm1*-(TBC-LRS). The cDNA encoding the mouse *Fkbp1a*/*Fkbp12* (amino acid residues 2 to 108) was cloned by using the

conventional PCR techniques and the following pair of oligonucleotides with a BamHI linker or a BglII linker (underlined): 5′-GGATCCGGAGTGCAGGTGGAGACCATC-3′ and 5′-AGATCTTCCTTCCAGTTTTAGAAGCTCCA-3′. Site-directed mutagenesis (i.e., F37M of FKBP1A) was performed by the PCR sewing methods essentially as described previously[37] and by using the following pair of oligonucleotides 5′-GATGGAAAGAAAATGGATTCCTCTCGG-3′ and 5′-CCGAGAGGAATCCATTTTCTTTCCATC-3′. The purified PCR product, FKBP1A[F37M] (named FM1), was directly inserted into the pGEM-T EASY vector (Promega, A1360). The FM insert was excised from the pGEM-T-FM1 by BamHI/SpeI double digestion and subcloned into the BglII/SpeI site of the pGEM-T-FM1. The resulting plasmid contained FM1 in tandem (named pGEM-T-FM2). This procedure was repeated 3 times and pGEM-T-FM4 was obtained (see Fig. S4A for details). The cDNA fragments of FM1, FM2, and FM4 were fused to the 5′-region of *Tbc1d25*ΔN cDNA to obtain FM1-*Tbc1d25*ΔN, FM2-*Tbc1d25*ΔN, and FM4-*Tbc1d25*ΔN, which were then inserted into the pMRX-IRES-puro-EGFP vector by the standard molecular biology techniques. pMRX-IRES-bsr-HA-ULK1 was similarly produced from pEF-HA-ULK1.[40] The cDNA insert of pEGFP-C1-TBC1D2B and pEF-T7-TBC1D5[20] was also subcloned into the pMRX-IRES-puro-HA vector[38] and pEF-FLAG tag vector.[39]

Immunofluorescence and image analyses

Immunofluorescence analysis was performed essentially as described previously.[20,22] In brief, cultured cells were fixed with 4% paraformaldehyde and stained with the specific antibodies indicated in each figure. The stained cells were examined for fluorescence with a confocal fluorescence microscope (Fluoview 1000; Olympus, Tokyo, Japan) through an objective lens (× 100 magnification, NA 1.45; Olympus) and with fluoview software (version 2.1c; Olympus). For quantitative analysis, images of the cells were captured at random with the confocal microscope, and the number of LC3 dots was counted with ImageJ software (version 1.43u; National Institutes of Health). The localization of SQSTM1 and TBC1D25 mutants in the ULK1-positive autophagosome initiation site in wortmannin-treated cells was investigated essentially as described previously.[19]

Immunoblot analysis

Immunoblot analysis was essentially performed as described previously.[39] Lysates of MEF cells were prepared with a lysis buffer (50 mM HEPES-KOH, pH 7.2, 150 mM NaCl, 1 mM MgCl$_2$, 1% Triton X-100 [Wako Pure Chemical Industries, Ltd., 169–21105], 1 mM DTT, protease inhibitors [0.1 mM PMSF, 10 μM leupeptin, and 10 μM pepstatin A]). The lysates were subjected to SDS-PAGE and transferred to a polyvinylidene difluoride membrane (MERCK Millipore, IPVH00010) by electroblotting. The membrane was blocked with 1% skim milk and 0.1% Tween-20 (Wako Pure Chemical Industries, Ltd., 166–21115) in phosphate-buffered saline (8 g/L NaCl, 0.36g/L KCl, 1.44 g/L NaH$_2$PO$_4$, NaKHPO$_4$ 0.24 g/L) followed by immunoblotting with the specific primary antibodies indicated in each

figure. Immunoreactive bands were visualized with appropriate HRP-conjugated secondary antibodies and detected by enhanced chemiluminescence. The blots shown in this paper are representative of at least 3 independent experiments.

GST (glutathione S-transferase) affinity isolation assay

GST affinity isolation assays were performed as described previously.[41,42] In brief, GST fusion proteins (GST-LC3B, GST-GABARAP, and GST-GABARAPL2)[20] were expressed and purified with glutathione-Sepharose beads (GE Healthcare, 17075605) by a standard protocol.[42] COS-7 cells transiently expressing EGFP-tagged TBC1D25 proteins (EGFP-TBC1D25, EGFP-TBC1D25-WA, or EGFP-TBC1D25-(SQT-LRS)) were homogenized in the lysis buffer and their lysates were obtained by centrifugation at $17,400 \times g$ for 10 min at $4°C$. A 75 μl volume of glutathione-Sepharose beads (wet volume) coupled with 15 μg of GST-fusion proteins (or GST alone) was incubated at $4°C$ for 1 h with 200 μl of COS-7 cell lysates containing each TBC1D25 protein. After washing the beads 3 times with 1 ml of the washing buffer (50 mM HEPES-KOH, pH 7.2, 150 mM NaCl, 1 mM $MgCl_2$, 1% Triton X-100, 1 mM DTT, protease inhibitors), proteins trapped with the beads were analyzed by SDS-PAGE, transferred to a polyvinylidene difluoride membrane, and then immunoblotted with anti-GFP antibody and HRP-conjugated anti-GST antibody.

Immunoprecipitation

COS-7 cells were transfected with pEF-T7-TBC1D25, pEF-FLAG-TBC1D25, pEF-T7-PB1-TBC1D25ΔN, pEF-FLAG-PB1-TBC1D25ΔN, pEF-T7-TBC1D2B, pEF-FLAG-TBC1D2B, pEF-T7-TBC1D5, pEF-FLAG-TBC1D5, pEF-T7-SQSTM1, pEF-FLAG-SQSTM1, or T7-GST, cultured for 2 d, and harvested. Immunoprecipitation assays with anti-T7 tag antibody-conjugated agarose were essentially performed as described previously.[43] In brief, beads that had been coupled with T7-tagged proteins were incubated with COS-7 cell lysates containing FLAG-tagged TBC1D25, PB1-TBC1D25ΔN, TBC1D2B, TBC1D5, or SQSTM1, and the proteins bound to the beads were analyzed by SDS-PAGE followed by immunoblotting with HRP-conjugated anti-FLAG tag antibody and HRP-conjugated anti-T7 tag antibody.

Electron microscopy analysis

Wild-type MEF cells expressing EGFP-TBC1D25 or EGFP-LC3, and *sqstm1*-KO MEF cells expressing EGFP-SQSTM1 or EGFP-PB1-TBC1D25ΔN were fixed with 4% paraformaldehyde and 0.05% or 0.1% glutaraldehyde in phosphate buffer, pH 7.4, and ultrathin cryosections were examined by immuno-electron microscopy essentially as described previously.[44] Rabbit polyclonal antibody against GFP (Abcam, ab6556) and donkey anti-rabbit IgG conjugated with 12-nm colloidal gold particles (Jackson ImmunoResearch laboratories, Inc., 711-205-152) were used as the primary and secondary antibodies, respectively. The sections were viewed with an electron microscope (JEM1200; JEOL). Colloidal gold particles on the inner membrane and outer membrane of autophagosomes were counted, and the percentage of outer membrane-localized particles (mean $\pm$ SE) is reported in the text.

Abbreviations

ATG	autophagy-related
BafA1	bafilomycin A_1
FKBP1A/FKBP12	FK506 binding protein 1A
FM	Phe-to-Met substitution at amino acid position 37 of FKBP1A
GAP	GTPase-activating protein
GST	glutathione *S*-transferase
HRP	horseradish peroxidase
KO	knockout
MAP1LC3/LC3	microtubule-associated protein 1 light chain 3
LRS	LC3 recognition sequence
MEF	mouse embryonic fibroblast
PB1	Phox and Bem1p
SQSTM1/SQT	sequestosome 1
TBC	Tre-2/Bub2/Cdc16
UBA	ubiquitin-associated
WT	wild type

Disclosure of potential conflicts of interest

No potential conflicts of interest were disclosed.

References

1. Mizushima N. Autophagy: process and function. Genes Dev 2007; 21:2861-73; PMID:18006683; http://dx.doi.org/10.1101/gad.1599207
2. Reggiori F, Klionsky DJ. Autophagy in the eukaryotic cell. Eukaryotic Cell 2002; 1:11-21; PMID:12455967; http://dx.doi.org/10.1128/EC.01.1.11-21
3. Suzuki K, Ohsumi Y. Molecular machinery of autophagosome formation in yeast, *Saccharomyces cerevisiae*. FEBS Lett 2007; 581:2156-61; PMID:17382324; http://dx.doi.org/10.1016/j.febslet.2007.01.096
4. Kabeya Y, Mizushima N, Ueno T, Yamamoto A, Kirisako T, Noda T, Kominami E, Ohsumi Y, Yoshimori T. LC3, a mammalian homologue of yeast Apg8p, is localized in autophagosome membranes after processing. EMBO J 2000; 19:5720-8; PMID:11060023; http://dx.doi.org/10.1093/emboj/19.21.5720
5. Mizushima N, Yoshimori T, Ohsumi Y. The role of Atg proteins in autophagosome formation. Annu Rev Cell Dev Biol 2011; 27:107-32; PMID:21801009; http://dx.doi.org/10.1146/annurev-cellbio-092910-154005
6. Fujita N, Hayashi-Nishino M, Fukumoto H, Omori H, Yamamoto A, Noda T, Yoshimori T. An Atg4B mutant hampers the lipidation of

LC3 paralogues and causes defects in autophagosome closure. Mol Biol Cell 2008; 19:4651-9; PMID:18768752; http://dx.doi.org/10.1091/mbc.E08-03-0312

7. Sou Y, Waguri S, Iwata J, Ueno T, Fujimura T, Hara T, Sawada N, Yamada A, Mizushima N, Uchiyama Y, et al. The Atg8 conjugation system is indispensable for proper development of autophagic isolation membranes in mice. Mol Biol Cell 2008; 19:4762-75; PMID:18768753; http://dx.doi.org/10.1091/mbc.E08-03-0309

8. Behrends C, Sowa ME, Gygi SP, Harper JW. Network organization of the human autophagy system. Nature 2010; 466:68-76; PMID:20562859; http://dx.doi.org/10.1038/nature09204

9. Wild P, McEwan DG, Dikic I. The LC3 interactome at a glance. J Cell Sci 2013; 127:3-9; PMID:24345374; http://dx.doi.org/10.1242/jcs.140426

10. Ichimura Y, Kumanomidou T, Sou YS, Mizushima T, Ezaki J, Ueno T, Kominami E, Yamane T, Tanaka K, Komatsu M. Structural basis for sorting mechanism of p62 in selective autophagy. J Biol Chem 2008; 283:22847-57; PMID:18524774; http://dx.doi.org/10.1074/jbc.M802182200

11. Okamoto K. Organellophagy: Eliminating cellular building blocks via selective autophagy. J Cell Biol 2014; 205:435-45; PMID:24862571; http://dx.doi.org/10.1083/jcb.201402054

12. Rogov V, Dötsch V, Johansen T, Kirkin V. Interactions between autophagy receptors and ubiquitin-like proteins form the molecular basis for selective autophagy. Mol Cell 2014; 53:167-78; PMID:24462201; http://dx.doi.org/10.1016/j.molcel.2013.12.014

13. Kirkin V, McEwan DG, Novak I, Dikic I. A role for ubiquitin in selective autophagy. Mol Cell 2009; 34:259-69; PMID:19450525; http://dx.doi.org/10.1016/j.molcel.2009.04.026

14. Fujita N, Yoshimori T. Ubiquitination-mediated autophagy against invading bacteria. Curr Opin Cell Biol 2011; 23:492-7; PMID:21450448; http://dx.doi.org/10.1016/j.ceb.2011.03.003

15. Itakura E, Kishi-Itakura C, Koyama-Honda I, Mizushima N. Structures containing Atg9A and the ULK1 complex independently target depolarized mitochondria at initial stages of parkin-mediated mitophagy. J Cell Sci 2012; 125:1488-99; PMID:19223761; http://dx.doi.org/10.1242/jcs.094110

16. Kageyama S, Omori H, Saitoh T, Sone T, Guan J-L, Akira S, Imamoto F, Noda T, Yoshimori T. The LC3 recruitment mechanism is separate from Atg9L1-dependent membrane formation in the autophagic response against Salmonella. Mol Biol Cell 2011; 22:2290-300; PMID:21525242; http://dx.doi.org/10.1091/mbc.E10-11-0893

17. Fujita N, Morita E, Itoh T, Tanaka A, Nakaoka M, Osada Y, Umemoto T, Saitoh T, Nakatogawa H, Kobayashi S, et al. Recruitment of the autophagic machinery to endosomes during infection is mediated by ubiquitin. J Cell Biol 2013; 203:115-28; PMID:24100292; http://dx.doi.org/10.1083/jcb.201304188

18. Klionsky DJ, Abdalla FC, Abeliovich H, Abraham RT, Acevedo-Arozena A, Adeli K, Agholme L, Agnello M, Agostinis P, Aguirre-Ghiso JA, et al. Guidelines for the use and interpretation of assays for monitoring autophagy. Autophagy 2012; 8:445-544; PMID:22966490; http://dx.doi.org/10.4161/auto.19496

19. Itakura E, Mizushima N. p62 targeting to the autophagosome formation site requires self-oligomerization but not LC3 binding. J Cell Biol 2011; 192:17-27; PMID:21220506; http://dx.doi.org/10.1083/jcb.201009067

20. Itoh T, Kanno E, Uemura T, Waguri S, Fukuda M. OATL1, a novel autophagosome-resident Rab33B-GAP, regulates autophagosomal maturation. J Cell Biol 2011; 192:839-53; PMID:21383079; http://dx.doi.org/10.1083/jcb.201008107

21. Fukuda M. TBC proteins: GAPs for mammalian small GTPase Rab? Biosci Rep 2011; 31:159-68; PMID:21250943; http://dx.doi.org/10.1042/BSR20100112

22. Itoh T, Fujita N, Kanno E, Yamamoto A, Yoshimori T, Fukuda M. Golgi-resident small GTPase Rab33B interacts with Atg16L and modulates autophagosome formation. Mol Biol Cell 2008; 19:2916-25; PMID:18448665; http://dx.doi.org/10.1091/mbc.E07-12-1231

23. Itoh T, Satoh M, Kanno E, Fukuda M. Screening for target Rabs of TBC (Tre-2/Bub2/Cdc16) domain-containing proteins based on their Rab-binding activity. Genes Cells 2006; 11:1023-37; PMID:16923123; http://dx.doi.org/10.1111/j.1365-2443.2006.00997.x

24. Söding J. Protein homology detection by HMM-HMM comparison. Bioinformatics 2005; 21:951-60; PMID:15531603; http://dx.doi.org/10.1093/bioinformatics/bti125

25. Bjørkøy G, Lamark T, Brech A, Outzen H, Perander M, Overvatn A, Stenmark H, Johansen T. p62/SQSTM1 forms protein aggregates degraded by autophagy and has a protective effect on huntingtin-induced cell death. J Cell Biol 2005; 17:603-14; PMID:16286508; http://dx.doi.org/10.1083/jcb.200507002

26. Rivera VM, Wang X, Wardwell S, Courage NL, Volchuk A, Keenan T, Holt DA, Gilman M, Orci L, Cerasoli F Jr, et al. Regulation of protein secretion through controlled aggregation in the endoplasmic reticulum. Science 2000; 287:826-30; PMID:10657290; http://dx.doi.org/10.1126/science.287.5454.826

27. Sumimoto H, Kamakura S, Ito T. Structure and function of the PB1 domain, a protein interaction module conserved in animals, fungi, amoebas, and plants. Sci STKE 2007; 2007(401):re6; PMID:17726178; http://dx.doi.org/10.1126/stke.4012007re6

28. Kishi-Itakura C, Koyama-Honda I, Itakura E, Mizushima N. Ultrastructural analysis of autophagosome organization using mammalian autophagy-deficient cells. J Cell Sci 2014; 127:4089-102; PMID:25052093; http://dx.doi.org/10.1242/jcs.156034

29. Mancias JD, Wang X, Gygi SP, Harper JW, Kimmelman AC. Quantitative proteomics identifies NCOA4 as the cargo receptor mediating ferritinophagy. Nature 2014; 509:105-9; PMID:24695223; http://dx.doi.org/10.1038/nature13148

30. Popovic D, Akutsu M, Novak I, Harper JW, Behrends C, Dikic I. Rab GTPase-activating proteins in autophagy: regulation of endocytic and autophagy pathways by direct binding to human ATG8 modifiers. Mol Cell Biol 2012; 2:1733-44; PMID:22354992; http://dx.doi.org/10.1128/MCB.06717-11

31. Pankiv S, Alemu EA, Brech A, Bruun J-A, Lamark T, Øvervatn A, Bjørkøy G, Johansen T. FYCO1 is a Rab7 effector that binds to LC3 and PI3P to mediate microtubule plus end-directed vesicle transport. J Cell Biol 2010; 188:253-69; PMID:20100911; http://dx.doi.org/10.1083/jcb.200907015

32. Birgisdottir ÅB, Lamark T, Johansen T. The LIR motif – crucial for selective autophagy. J Cell Sci 2013; 126:3237-47; PMID:23908376; http://dx.doi.org/10.1242/jcs.126128

33. Kirkin V, Lamark T, Sou YS, Bjørkøy G, Nunn JL, Bruun JA, Shvets E, McEwan DG, Clausen TH, Wild P, et al. A role for NBR1 in autophagosomal degradation of ubiquitinated substrates. Mol Cell 2009; 33:505-16; PMID:19250911; http://dx.doi.org/10.1016/j.molcel.2009.01.020

34. Fukuda M, Mikoshiba K. A novel alternatively spliced variant of synaptotagmin VI lacking a transmembrane domain: Implications for distinct functions of the two isoforms. J Biol Chem 1999; 274:31428-34; PMID:10531344; http://dx.doi.org/10.1074/jbc.274.44.31428

35. Komatsu M, Waguri S, Koike M, Sou YS, Ueno T, Hara T, Mizushima N, Iwata J, Ezaki J, Murata S, et al. Homeostatic levels of p62 control cytoplasmic inclusion body formation in autophagy-deficient mice. Cell 2007; 131:1149-63; PMID:18083104; http://dx.doi.org/10.1016/j.cell.2007.10.035

36. Morita S, Kojima T, Kitamura T. Plat-E: an efficient and stable system for transient packaging of retroviruses. Gene Ther 2000; 7:1063-6; PMID:10871756; http://dx.doi.org/10.1038/sj.gt.3301206

37. Kobayashi H, Fukuda M. Rab35 regulates Arf6 activity through centaurin-β2 (ACAP2) during neurite outgrowth. J Cell Sci 2012; 125:2235-43; PMID:22344257; http://dx.doi.org/10.1242/jcs.098657

38. Saitoh T, Nakayama M, Nakano H, Yagita H, Yamamoto N, Yamaoka S. TWEAK induces NF-κB2 p100 processing and long lasting NF-κB activation. J Biol Chem 2003; 278:36005-12; PMID:12840022; http://dx.doi.org/10.1074/jbc.M304266200

39. Fukuda M, Kanno E, Mikoshiba K. Conserved N-terminal cysteine motif is essential for homo- and heterodimer formation of synaptotagmins III, V, VI, and X. J Biol Chem 1999; 274:31421-7; PMID:10531343; http://dx.doi.org/10.1074/jbc.274.44.31421

40. Ishibashi K, Uemura T, Waguri S, Fukuda M. Atg16L1, an essential factor for canonical autophagy, participates in hormone secretion

from PC12 cells independently of autophagic activity. Mol Biol Cell 2012; 23:3193-202; PMID:22740627; http://dx.doi.org/10.1091/mbc. E12-01-0010

41. Kuroda TS, Fukuda M, Ariga H, Mikoshiba K. The Slp homology domain of synaptotagmin-like proteins 1-4 and Slac2 functions as a novel Rab27A binding domain. J Biol Chem 2002; 277:9212-8; PMID:11773082; http://dx.doi.org/10.1074/jbc. M112414200

42. Kuroda TS, Fukuda M. Identification and biochemical analysis of Slac2-c/MyRIP as a Rab27A-, myosin Va/VIIa-, and actin-binding

protein. Methods Enzymol 2005; 403:431-44; PMID:16473609; http://dx.doi.org/10.1016/S0076-6879(05)03038-7

43. Fukuda M, Kanno E. Analysis of the role of Rab27 effector Slp4-a/granuphilin-a in dense-core vesicle exocytosis. Methods Enzymol 2005; 403:445-57; PMID:16473610; http://dx.doi.org/10.1016/S0076-6879(05)03039-9

44. Waguri S, Komatsu M. Biochemical and morphological detection of inclusion bodies in autophagy-deficient mice. Methods Enzymol 2009; 453:181-96; PMID:19216907; http://dx.doi.org/10.1016/S0076-6879(08)04009-3